

# Secondary defects engineering in *c*-Si: Influence of implantation dose, temperature, and oxygen concentration

R. Poirier,<sup>a)</sup> F. Schiettekatte, S. Roorda, and M. O. Fortin

Groupe de recherche en physique et technologie des couches minces et Département de physique,  
Université de Montréal, Montréal, Québec, Canada, H3C 3J7

(Received 13 August 1999; accepted 15 August 1999)

The influence of implantation temperature, dose, and oxygen concentration was investigated for 230 keV phosphorus implantation in crystalline silicon. It was found that oxygen impurities act as nucleation centers for extended defects, which increases their density in O-rich samples compared to conventional *c*-Si. For doses below  $2 \times 10^{14}$  P/cm<sup>2</sup>, the density of extended defects varies rapidly with dose and depends weakly on implantation temperature while for higher doses, the extended defect density varies linearly with dose and depends strongly on implantation temperature. Using a simple criterion for extended defect formation, the dose at which temperature control of extended defects becomes efficient is evaluated for several ion species and energies. © 2000 American Vacuum Society. [S0734-2101(00)03902-6]

## I. INTRODUCTION

Doping of semiconductor materials using ion implantation is a standard processing step for silicon based microelectronic devices. This process followed by high temperature annealing of the implanted material also leads to the clustering of primary point defects (PD) into extended secondary defects (XD) such as dislocation loops and rod-like defects.<sup>1-3</sup> Extended defects have detrimental effects on device performance<sup>4</sup> such as a reduction of carrier lifetime and large leakage currents. Control of XD density in postannealed implanted material is therefore imperative to achieve desirable performance.

In previous work, Schreutelkamp *et al.*<sup>1</sup> have related the onset of XD creation to the areal density of displaced silicon atoms. Above a critical value, called the threshold dose, the amount of damage is sufficiently high so that the primary defects do not completely annihilate during annealing and coalesce into extended structures. Consequently, changing the amount and type of the primary defects will result in changes in XD formation.<sup>4</sup> The structure of primary defects is influenced by (i) mass of implanted ion, (ii) implantation energy, (iii) wafer temperature, (iv) implant dose, (v) ion flux, and (vi) beam orientation (channeled versus random). Controlling threshold dose has already been achieved by increasing the implantation temperature and reducing the ion flux. Other methods include cycles of subthreshold implantation followed by annealing<sup>4</sup> that allows the doping of wafers to doses above threshold without introduction of XD.

In order to further investigate the influence of implantation temperature on secondary defect formation, we have studied the areal XD density (defects/cm<sup>2</sup>) using both transmission electron microscopy (TEM) and chemical etching followed by optical microscopy for room-temperature (RT) (23 °C), 150 °C, and 300 °C at implant doses near threshold. Since temperature affects dynamic recombination of primary defects during implantation, it is likely that it modifies sig-

nificantly the processes during subsequent annealing such as cluster formation and XD nucleation.

## II. EXPERIMENTAL METHOD

230 keV <sup>31</sup>P<sup>+</sup> ions were implanted to 15 different doses ranging from  $0.6 \times 10^{14}$  to  $5 \times 10^{14}$  P/cm<sup>2</sup>, using a 1.7 MV Tandem accelerator at the Université de Montréal, into undoped *n*-type Czochralski-grown (Cz) silicon wafers with  $\langle 100 \rangle$  orientation tilted 7° from axis to avoid channeling. Such doses are below the amorphization dose of Si by 230 keV P<sup>+</sup> ions. A set of  $\langle 100 \rangle$  wafers with high oxygen content ( $\sim 10^{18}$  cm<sup>-3</sup>) was also implanted. The beam current was maintained approximately at 100 nA/cm<sup>2</sup> during implantation. Each series of implantations were carried out at three different wafer temperatures RT (23 °C), 150 °C, and 300 °C. The samples were subsequently annealed in a rapid thermal annealing system [(RTA), Minipulse A. G. Associates] at 1000 °C for 30 s (rise time 8 s, cooling time 5 s to 500 °C) under N<sub>2</sub> atmosphere to create extended defects.

The density of XD was evaluated using two different methods, a chemical etching technique for low XD densities and transmission electron microscopy for high densities. The former technique used an etchant (Wright etch<sup>6</sup>) that delineates XD. Evaluation of the defect density is afterwards simply done under an optical microscope. This method is however limited to densities under  $\sim 2 \times 10^7$  XD/cm<sup>2</sup> due to the dimensions of the etch pits.

For higher defect densities, plan-view transmission electron microscopy was used to determine the XD areal density. Annealed samples were first thinned down to 20 μm by mechanical polishing and were further thinned by Ar sputtering to electron transparency. The samples were then studied both in bright and dark field modes with a 300 kV Philips CM-30 TEM.

## III. INFLUENCE OF DOSE AND TEMPERATURE

Figure 1 summarizes our results. The vertical axis represents the areal defect density (XD/cm<sup>2</sup>) as measured with

<sup>a)</sup>Electronic mail: poirier@lps.umontreal.ca

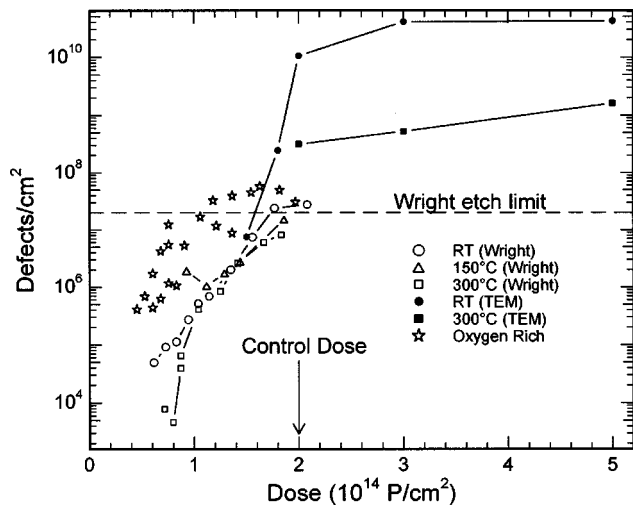


Fig. 1. Areal density of extended defects as measured by Wright etch delineation (open symbols) and direct TEM measurements (solid symbols) vs dose for RT, 150 °C, and 300 °C 230 keV P implantations of (100) c-Si and O-rich c-Si (crosses). O-rich Si exhibits a higher XD density than normally Cz-grown Si. The arrow indicates the ion dose above which the implantation temperature helps to reduce the postanneal XD density.

Wright etch delineation technique (open symbols) and direct TEM observation (solid symbols) for three different implantation temperatures: room temperature (RT), 150 °C, and 300 °C.

Two different regions can be identified in Fig. 1; low doses ( $<2 \times 10^{14} \text{ cm}^{-2}$ ) for which we observe a steep increase of 5 orders of magnitude in XD density which constitutes the so-called threshold dose, and high doses ( $>2 \times 10^{14} \text{ cm}^{-2}$ ) where the XD density stabilizes close to a linear increase. At high doses, the substrate temperature has a strong influence on defect nucleation, the XD density of high temperature implants being one order of magnitude lower than RT implants. In the low dose range, the substrate temperature influence is somewhat attenuated, probably because the density of primary defects is too low to influence their nucleation into XD even at elevated temperature. The apparent mismatch between Wright etch and TEM data is due to the fact that the surface of etched samples was saturated with etch pits for doses above  $1.8 \times 10^{14} \text{ P/cm}^2$ , leading to an underestimation of the defect density. Nonetheless, at least one TEM data point ( $1.5 \times 10^{14} \text{ P/cm}^2$ , RT) falls into the range of Wright etch data, which suggest the concordance of the two methods.

Figure 2 presents two TEM plan-view micrographs of c-Si implanted with  $3 \times 10^{14} \text{ P/cm}^2$  at RT and 300 °C, annealed in RTA. A high areal density of small Frank loops ( $\sim 30 \text{ nm}$ ) is observed in the RT sample, while a low density of large dislocation loops ( $\sim 120 \text{ nm}$ ) is observed for 300 °C implants. The ratio of interstitials in these defects, measured from the TEM pictures, to the implanted dose is about 1.2 for RT at all doses, 0.4 for 300 °C for doses of  $2 \times 10^{14}$  and  $3 \times 10^{14} \text{ P/cm}^2$ , and reaches 1.0 for  $5 \times 10^{14} \text{ P/cm}^2$ . Our RT data compare well with data in literature<sup>5</sup> showing a slight positive deviation from the “+1” model, which states that

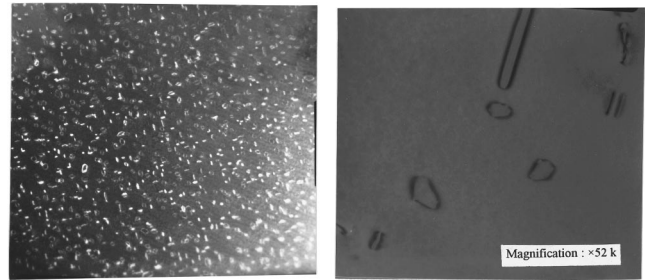


Fig. 2. TEM plan-view micrographs (same magnification) of normal Cz Si samples implanted at  $3 \times 10^{14} \text{ P/cm}^2$  at RT (left) and 300 °C (right).

all interstitials and holes created by the collision cascade annihilate with each other during the anneal, leaving only one interstitial per implanted ion. It is interesting to note the interstitial imbalance for higher temperature implantation that suggests that significant deviation from the +1 model is dependent on the implant temperature as well as on the ion mass.<sup>7,8</sup>

#### IV. INFLUENCE OF OXYGEN

Implantations of Cz-grown Si containing a high level ( $\sim 10^{18} \text{ cm}^{-3}$ ) of oxygen were also performed. Such high O concentration is employed for specific applications such as the creation of denuded zones for internal impurity gettering during device processing.<sup>9</sup> O impurities have a strong effect on the nucleation of primary defects into XD. Figure 1 shows the areal etch pit density of O-rich samples for several temperature (stars). The oxygen impurities in the crystal serve as nucleation centers favoring the coalescence of PD into extended structures, hence the areal etch pit density (etch pit/cm<sup>2</sup>) measured on such O-rich wafers was several times higher than in normal Si. Scattering of the O-rich Si data is due to the fluctuation in O content over the wafer area. Regions of different O-impurity concentration could easily be identified by the naked eye as concentric circles across the wafer after etching. Despite the very strong effect of oxygen, the XD density still increased 100 fold between  $0.4 \times 10^{14}$  and  $2 \times 10^{14} \text{ ions/cm}^2$ , which confirms the important role of the PD concentration in XD nucleation.

#### V. DEFECT ENGINEERING

Our results show that for 230 keV P implants, increasing the substrate temperature only reduces the XD density for doses higher than  $2 \times 10^{14} \text{ P/cm}^2$ . Using Schreutelkamp’s argument that secondary defect formation is dependent on the total number of displaced silicon atoms above a certain threshold<sup>1</sup> and TRIM (98.01) simulations,<sup>10</sup> we can estimate for various ions and energies the dose at which implantation temperature is efficient in controlling XD formation. The result of the control dose estimation is illustrated in Fig. 3. As the energy and mass of the implanted ion increase, the amount of damage per ion introduced in the material increases, thus the control dose should decrease accordingly.

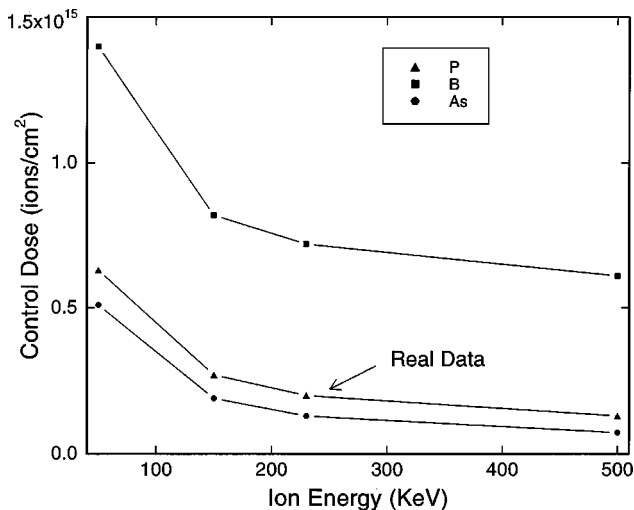


FIG. 3. Calculation using TRIM (98.01) of the dose at which temperature control of XD becomes efficient. The point corresponding to P 230 keV is our experimental data point from which the others are estimated.

## VI. CONCLUSIONS

Our results have shown that the substrate temperature during ion implantation has an important effect on nucleation of PD into extended defects structures, reducing the XD density by one order of magnitude at high doses. In the lower dose range, the XD density exhibits a weaker dependence on temperature. In addition to reducing the XD density, high temperature implants change the structure of the defects; the size of postanneal dislocation loops, as seen with plan-view TEM, changes from 30 nm for RT implants to more than 100 nm for 300 °C implants. TEM data indicate significant deviations from the +1 annealing model; and show a dependence on implant temperature and not solely on ion mass. Impurities such as oxygen act as nucleation centers that greatly enhance the creation of XD.

The control of XD creation during device processing is critical to achieve optimal device performance. Our results show that high temperature implantation reduces the XD density for high doses implantations such as those required for doping. Using Schreutelkamp's criterion for the formation of XD, it is possible to evaluate the dose at which temperature control of defects becomes efficient for a variety of ion masses and energies.

## ACKNOWLEDGMENTS

The authors are grateful to P. Bérichon and R. Gosselin for technical assistance with the operation of the Tandem accelerator as well as L. Isnard for RTA operation and the help of M. Chicoine on TEM techniques. This work was financially supported by grants from the Natural Sciences and Engineering Research Council of Canada (NSERC) and Le Fonds pour la Formation de Chercheurs et l'Aide à la Recherche (Fonds FCAR) du Québec.

- <sup>1</sup>R. J. Schreutelkamp, J. S. Custer, J. R. Liefting, W. X. Lu, and F. W. Saris, *Mater. Sci. Rep.* **6**, 275 (1991).
- <sup>2</sup>J. L. Benton, S. Libertino, P. Kringhøj, D. J. Eaglesham, and J. M. Poate, *J. Appl. Phys.* **82**, 120 (1997).
- <sup>3</sup>J. Li and K. S. Jones, *Appl. Phys. Lett.* **73**, 3748 (1998).
- <sup>4</sup>J. R. Liefting, Ph.D. thesis, University of Twente, The Netherlands, 1992 (unpublished); J. R. Liefting, J. S. Custer, R. J. Schreutelkamp, and F. W. Saris, *Mater. Sci. Eng., B* **15**, 173 (1992).
- <sup>5</sup>P. A. Stolk, H. J. Grossmann, D. J. Eaglesham, D. C. Jacobson, C. S. Rafferty, G. H. Gilmer, M. Jaraiz, J. M. Poate, H. S. Luftman, and T. E. Haynes, *J. Appl. Phys.* **81**, 6031 (1997).
- <sup>6</sup>M. Wright Jenkins, *J. Electrochem. Soc.* **124**, 757 (1977).
- <sup>7</sup>S. B. Herner, H. J. Grossmann, L. P. Pelaz, G. H. Gilmer, M. Jaraiz, D. C. Jacobson, and D. J. Eaglesham, *J. Appl. Phys.* **83**, 6182 (1998).
- <sup>8</sup>F. Schiettekatte, S. Roorda, R. Poirier, M. O. Fortin, S. Chazal, and R. Héliou, *Nucl. Instrum. Methods Phys. Res. B* (in press).
- <sup>9</sup>G. Obermeier, J. Hage, and D. Huber, *J. Appl. Phys.* **82**, 595 (1997).
- <sup>10</sup>J. F. Ziegler, J. P. Biersack, and U. Littmark, *The Stopping Range of Ions in Solids* (Pergamon, New York, 1985).